

Holography-Inspired Screens for Sub-Wavelength Focusing in the Near Field

George V. Eleftheriades, *Fellow, IEEE*, and A. M. H. Wong

Abstract—Inspired by the principle of holography we present a concept for making simple transmission screens that can focus an incident wave into a sub-wavelength spot in the near field. The screen is made out of closely spaced, unequal slits cut on a metallic sheet. Fullwave simulations are presented for an example screen that focuses an incident plane wave down to a spot having a peak-to-null beamwidth equal to $\lambda/10$.

Index Terms—Diffraction limit, evanescent waves, holography, metamaterials, super-lenses.

I. INTRODUCTION

INSPIRED by the notion of the “perfect lens” proposed by J.B. Pendry [1] there have been many recent efforts to focus electromagnetic waves into sub-wavelength spots in the near field [2]–[4]. Such near-field focusing structures hold promise for improving microscopy, lithography, and near-field sensing and imaging, amongst other applications. A recent effort on this front was carried out by R. Merlin who proposed near-field focusing using an assumed aperture current distribution obtained by manipulating the corresponding plane-wave spectrum [5]. In this Letter we describe the results of a parallel effort in the authors’ group [6]. In contrast to [5], our efforts have been inspired by concepts from holography but applied to the near field, with a corresponding setup shown in Fig. 1. Our formulation goes beyond that of [5] in that it accounts for both propagating and evanescent waves and can handle any arbitrary incident wave. Unlike [5] which merely proposes generic screen current distributions, we hereby propose readily realizable holographic screen patterns that only require simple resonant slits of unequal length cut on a ground plane.

II. CONCEPT AND FORMULATION

The basic idea is to design a metallic transmission screen that will allow an incident plane wave $A_{inc}(x)$ to form a sub-wavelength focus on the other side of the screen (see Fig. 1). For this purpose, we need to determine a suitable “source” distribution at the image plane, a distance “ d ” from the screen. Since this should be a sub-wavelength distribution, it should contain ample evanescent-wave (near-field) components.

Therefore, we can choose source distributions of the form $\exp(-jkr)/r^n$, where n is an integer. Of course such source distributions are singular at $r = 0$ and cannot be possibly re-

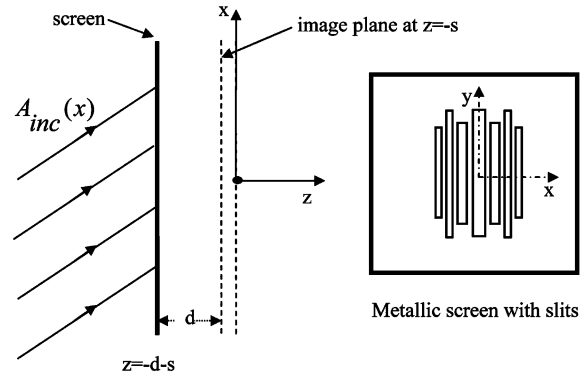


Fig. 1. Near-field focusing set up with a metallic screen.

constructed at the singularity point. Nevertheless, such a distribution can be potentially reconstructed at a nearby auxiliary plane, a distance “ s ” from $r = 0$ (see Fig. 1). We choose the following source distribution to reconstruct:

$$E_{source}(x, z = -s) = \frac{\exp(jkr)}{r}, \quad r = \sqrt{x^2 + s^2}. \quad (1)$$

For convenience, we have assumed 2D ($\partial/\partial y = 0$) and scalar propagation; Likewise, we have chosen only a $1/r$ field variation.

In fact, higher powers ($n > 1$) result in richer evanescent-wave spectrums. However, with our choice, we can analytically calculate the angular spectrum at the image plane which is:

$$\begin{aligned} S(k_x, z = -s) &= \int_{-\infty}^{+\infty} E_{source}(x) \exp(-jk_x x) dx \\ &= K_o(jsk_z) \end{aligned} \quad (2)$$

where $k_z = -j\sqrt{k_x^2 - k^2}$ and K_o is the modified Bessel function of the second kind. From (2) it is evident that for $s \ll \lambda$ there is a finite evanescent-wave spectrum which approaches $K_o(k_x s)$ for $k_x \gg k$ and hence remains bounded.

The next step in our formulation is to determine the field distribution at the screen which corresponds to the image field (1). For this purpose, the corresponding spectrum (2) must be back-propagated to the screen plane by multiplying it with the factor $\exp(+jk_z d)$. For the propagating components, this process leads to a phase reversal $\exp(j|k_z|(d+s))$, whereas for the evanescent components leads to a growth which can be written for $k_x \gg k$ as,

$$S(k_x, z = -s - d) = K_o(|k_x|s) \exp(|k_x|(d+s)) \quad (3)$$

Equation (3) represents the evanescent-wave spectrum that needs to be established at the screen plane in order to re-

Manuscript received September 24 2007; revised December 6, 2007.

The authors are with the Edward S. Rogers, Sr. Department of Electrical and Computer Engineering, Toronto, ON M5S 3G4, Canada (e-mail: gelefth@waves.utoronto.ca).

Color versions of one or more of the figures in this letter are available online at <http://ieeexplore.ieee.org>.

Digital Object Identifier 10.1109/LMWC.2008.918871

construct the sub-wavelength focused beam (1) at the image plane. With this in mind, let us examine (3) more carefully: This spectrum is very rich in evanescent-wave components and although the Bessel term asymptotically attenuates as $\exp(-k_x s)$, there is an overall total growth of $\exp(k_x d)$ which becomes unbounded as $k_x \rightarrow \infty$. To this end, we need to make the original source spectrum band-limited so that the spectrum at the screen remains finite. Therefore, (2) and (3) should be thought of as vanishing outside the range $|k_x| \leq k_m$, where k_m is the maximum transverse wavenumber to be reconstructed. Consequently, k_m would ultimately determine the achieved sub-wavelength beamwidth (resolution) at the image plane. Since the overall spectrum is dominated by the large exponentially growing evanescent components, we can approximate the screen spectrum by its asymptotic form,

$$S(k_x, z = -s - d) \cong \exp(|k_x| d) \quad (4)$$

$$k_o < |k_x| \leq k_m.$$

We are now ready to determine the spatial distribution that needs to be established at the screen plane. For this purpose, one needs to inverse Fourier transform (4) in its band-limited version. In this way, and assuming that $k_m \gg k_0$ the following approximate expression for a field component that leads to sub-wavelength focusing can be obtained,

$$S_{apr}(x, z = -s - d) = e^{k_m d} \frac{\cos(k_m x)}{d^2 + x^2}. \quad (5)$$

We can now calculate the corresponding field distribution at the image plane. For this purpose, we first calculate the spectrum of (5) which is,

$$S_{apr}(k_x, z = -s - d) = e^{k_m d} \frac{\pi}{2d} \left[e^{-d|k_x - k_m|} + e^{-d|k_x + k_m|} \right]. \quad (6)$$

Using (6) the field at the image-plane is given by,

$$S_{apr}^{img}(x) = \int_{-\infty}^{+\infty} S_{apr}(k_x, z = -s - d) e^{-jk_z d} e^{-jk_x x} dk_x. \quad (7)$$

After some tedious algebra (7) can be approximated by,

$$S_{apr}^{img}(x) \cong \frac{\pi}{2d} \left[\frac{2d}{x^2 + 4d^2} + \frac{\sin(k_m x)}{x} \right]. \quad (8)$$

The dominant term in (8) is the second one which is a sub-wavelength *sinc* distribution of full-null beamwidth $2\pi/k_m$. The first term is just a weak background distribution. Moreover, by comparing (5) and (8), it can be noted that there is an exponential field attenuation $\exp(-k_m d)$ from the screen to the image plane (as expected). Fig. 2 compares the exact integration (7) with the approximate closed-form expression (8) showing excellent agreement.

Now for a given screen field distribution $S(x)$, we need to synthesize a transmission screen that will produce it upon illumination by a plane wave $A_{inc}(x)$ (see Fig. 1). For this purpose, we can invoke the holographic principle again and consider a transmission function that is proportional to the intensity of the interference pattern between $S(x)$ and the incident field at the

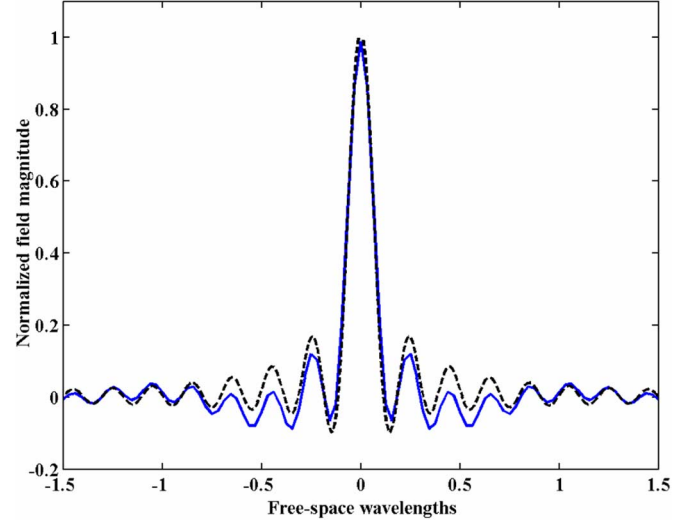


Fig. 2. Field at image plane, solid-line = exact integration (7), dashed-line = approximate expression (8).

screen $A_{inc}(x)$. The corresponding transmission function will then be,

$$T(x) \propto |S(x)|^2 + |A_{inc}(x)|^2 + S_{ap}^*(x)A_{inc}(x) + S_{ap}(x)A_{inc}^*(x). \quad (9)$$

A nice property of this holographic screen is that the incident wave can be arbitrary, as long as $|A_{inc}|$ is constant, such as a general oblique plane-wave or even a far-field spherical wave. Moreover, $T(x)$ is positive and real which facilitates its realization using slits cut on a ground plane. However, as always in holography, extraneous modes are produced which can obliterate the image if they are not properly filtered out [7]. To this end, our target screen distribution (5) is already real but assumes both positive and negative values. Therefore, we can attempt to synthesize (5) directly, upon a normally incident plane wave illumination, thus avoiding potential complications with holographic extraneous images. For this purpose, we can still use slits cut on a metallic sheet as will be discussed in the next section.

III. PHYSICAL SCREEN STRUCTURE AND RESULTS

Let us now deal with the problem of physically realizing (5) using an array of slits cut on a ground plane. A practical goal for an example structure, would be to allow evanescent-wave components up to $k_m = 5k = 2\pi/\lambda_m$, thus achieving a full-null-beamwidth of $\lambda/5$ at say $d = \lambda/10$ from the transmission screen. Without loss of generality, let us also assume that $f = 3$ GHz and thus $\lambda = 10$ cm in free space.

A. Ideal Slit Configuration

With the above assumptions let us synthesize (5) using two slits per λ_m wavelength (to satisfy the sampling theorem). Then we can place these slits at the discrete locations $x_n = \pm n\lambda_m/2 = \pm nd$ where $n = 0, 1, 2, 3 \dots$. From (5), the required (normalized) field strengths at each slit are therefore $S_n = (-1)^n/(1 + n^2) = 1, -1/2, +1/5, -1/10 \dots$. Fig. 3 shows the focused field distribution at the image plane for

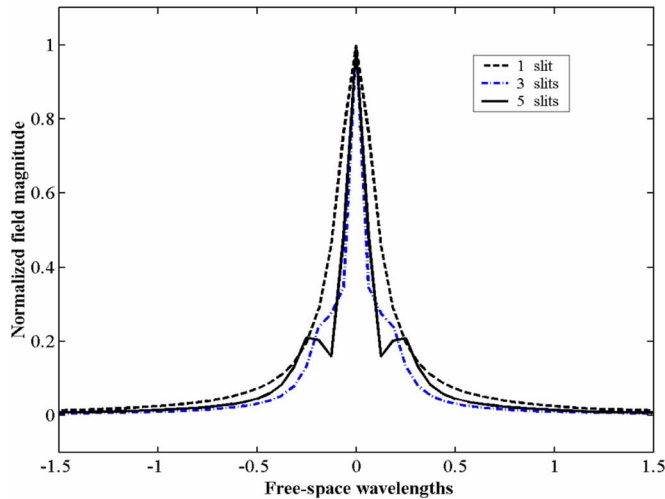


Fig. 3. Field distribution at image plane $d = \lambda/10$ for various numbers of slots of width $= S_n^* \lambda_m / 4$.

one, three, and five slits (assuming uniformly illuminated slits and an exact plane-wave expansion integration). As shown, with five slits a full-null beamwidth of $\lambda/5$ is achieved and a full 3dB beamwidth of $0.6^* \lambda/5$, as predicted by (8). This result along with Fig. 2 do validate the various assumptions and approximations that we have used so far. Moreover, Fig. 3 suggests that even with only three slits, a $\lambda/5$ resolution can be obtained.

B. Fullwave Simulations

To physically synthesize such a transmission screen, both positive and negative field amplitudes have to be realized. For this purpose, we can use slits close to resonance: Slits shorter than $\lambda/2$ are inductive whereas slits longer than $\lambda/2$ are capacitive. Therefore, we can create the required π phase shift by using adjacent inductive and capacitive slits. Furthermore, by changing the length and width of the slits, we can control the slit-field amplitude. Using this approach, we have designed a three-slit screen with Ansoft's HFSS. The result for a normally incident plane-wave is shown in Fig. 4, where a clear $\lambda/5$ full-null beamwidth is achieved (in contrast to the much wider beamwidth from a single slot, also at $d = \lambda/10$, see Fig. 3). A final note is that although there is a field attenuation of $\exp(-k_m d)$ from screen to image plane, nevertheless the field strengths of the incident and focused fields are comparable because the slits are almost resonant and hence the local

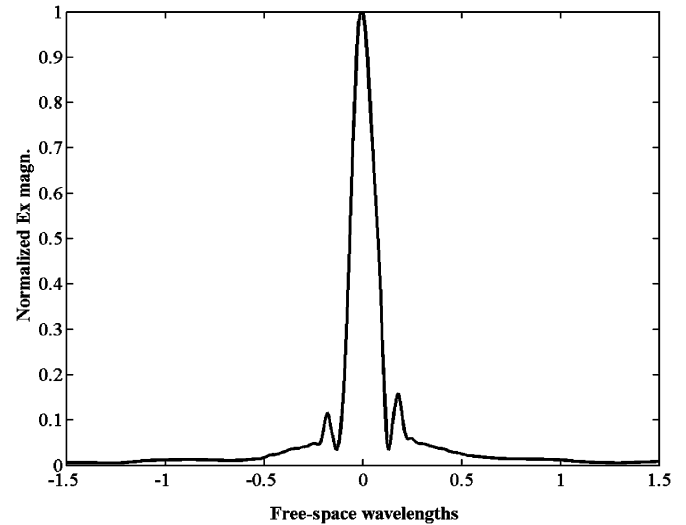


Fig. 4. Full-wave HFSS simulation of a three-slit screen at 3 GHz. The central slit has dimensions $53 \text{ mm} \times 4 \text{ mm}$ and the adjacent two $40 \text{ mm} \times 2.5 \text{ mm}$. By optimizing the slit widths a $\lambda/5$ full null beamwidth is achieved close to the ideal case of Fig. 2.

slit field is enhanced (compared to the incident field strength). Moreover, it should be pointed out that unlike the “perfect lens” [1], the beamwidth is not directly related to losses (only the focused field magnitude is affected but not the resolution). Finally if 2-D beams are desired, one can envision three concentric slits with a central off-resonant capacitive slit and then load inductively the interior and exterior ones using, for example, simple printed pads.

REFERENCES

- [1] J. B. Pendry, “Negative refraction makes a perfect lens,” *Phys. Rev. Lett.*, vol. 85, no. 18, pp. 3966–3969, Apr. 2000.
- [2] A. Salandrino and Engheta, “Far-field subdiffraction optical microscopy using metamaterial crystals: Theory and simulations,” *Phys. Rev. B*, vol. 74, pp. 075103–075103, Aug. 2006.
- [3] A. Grbic and G. V. Eleftheriades, “Overcoming the diffraction limit with a planar left-handed transmission-line lens,” *Phys. Rev. Lett.*, vol. 92, no. 11, pp. 117403–117403, Mar. 2004.
- [4] P. Alitalo, S. Maslovski, and S. Tretyakov, “Experimental verification of the key properties of a three-dimensional isotropic transmission-line superlens,” *J. Appl. Phys.*, vol. 99, pp. 124910–124910, 2006.
- [5] R. Merlin, “Radiationless electromagnetic interference: Evanescent-field lenses and perfect focusing,” *Science*, Jul. 2007.
- [6] G. V. Eleftheriades, “Negative-Refractive-Index transmission-line (NRI-TL) metamaterials,” in *Proc. Int. Symp. Electromagn. Theory URSI-Comm. B*, Ottawa, ON, Canada, Jul. 26–28, 2007, [CD ROM].
- [7] J. W. Goodman, *Introduction to Fourier Optics*. Englewood, CO: Roberts & Company, 2005.